Polyhedron 29 (2010) 3137–3145

Contents lists available at ScienceDirect

Polyhedron

journal homepage: www.elsevier.com/locate/poly

Syntheses and characterization of Cu^{2+}, Ni^{2+} and Zn^{2+} binding capability of histidinehydroxamic acid derivatives

Edit Csapó [a], Péter Buglyó [a], Nóra Veronika Nagy [b], M. Amélia Santos [c], Alma Corona [d], Etelka Farkas [a,*]

[a] Department of Inorganic and Analytical Chemistry, University of Debrecen, H-4010 Debrecen, Hungary
[b] Institute of Structural Chemistry, Chemical Research Center of the Hungarian Academy of Sciences, H-1525 P.O. Box 17, Budapest, Hungary
[c] Centro de Química Estrutural, Instituto Superior Técnico, 1049-001 Lisboa, Portugal
[d] Universidad de Guanajuato, Facultad de Quimica, Guanajuato, GTO. 36050, Mexico

ARTICLE INFO

Article history:
Received 13 July 2010
Accepted 19 August 2010
Available online 24 August 2010

Keywords:
Histidinehydroxamic acid derivatives
Cu^{2+}-, Ni^{2+}-, Zn^{2+}-complexes
Solution equilibrium
Potential metalloenzyme inhibitors

ABSTRACT

Two histidinehydroxamic acid derivatives (*N*-methyl-histidinehydroxamic acid, *N*-Me-Hisha and *Z*-histidinehydroxamic acid, *Z*-Hisha) have been synthesized and their complexation with Cu^{2+}-, Ni^{2+}- and Zn^{2+}-ions has been studied by using pH-potentiometric, UV–Vis, CD, ^{1}H NMR, EPR and ESI-MS methods. Both of the two new derivatives contain one donor atom less compared to the histidinehydroxamic acid (Hisha). In the case of *N*-Me-Hisha the hydroxamate-N as donor is eliminated, while the coordination of the amino-*N* of *Z*-Hisha is not possible at all.

With the ambidentate *N*-Me-Hisha, the histamine-type coordination mode is favoured if the metal ion is Ni^{2+} and the bis-[NH_2,N_{imid}] complex is the most stable in this system. The mixed type, [NH_2,N_{imid}] + [O,O], coordination mode dominates in the Cu^{2+}- *N*-Me-Hisha complexes, while different low stability mono-chelated linkage isomers are formed with Zn^{2+}.

With *Z*-Hisha (having poor water solubility) hydroxamate-type coordination mode predominates in low stability complexes in the Ni^{2+} and Zn^{2+} containing systems. Interestingly, the interaction with Cu^{2+} is very strong and results in the formation of a high stability 12-MC-4 type metallacrown with involvement of 5-membered and 7-membered chelates.

© 2010 Elsevier Ltd. All rights reserved.

1. Introduction

Selective inhibition of metalloenzymes is an area of intense interest because numerous serious diseases are correlated with the dysfunction of such type of enzymes. For example, the zinc-containing matrix metalloproteinases (MMPs) play a determinant role in the evolvement of arthritis, periodontal diseases, multiple sclerosis and also in the metastatic spread of various human cancers [1,2]. This is one reason why the selective inhibition of MMPs has become one of the prominent drug design targets for medicinal chemists. There is no doubt that the inhibitory effect is correlated with the chelation of the catalytic metal center, thereby the linkage of the substrate molecule is hindered [3,4]. Previous results related to zinc-containing histone deacetylases and MMPs, or nickel-containing ureases show that hydroxamic acids, which have good metal binding capability, are effective inhibitors of these enzymes [5–8]. Besides the metalloenzyme inhibitory effects with important roles in several pathological processes, antibiotic effects as well as metal ion sequestering ability of hydroxamic acids are also well-known and the crucial role of hydroxamate-based siderophores in the Fe^{3+} uptake, transfer and storage in the microorganisms via complexation is commonly known [9].

Since amino acid based and especially peptide based hydroxamic derivatives are often among the possible candidates as inhibitors for various metalloenzymes, it is interesting to know the main factors affecting the metal binding ability/binding mode of such molecules. In order to learn more about the stability, binding mode and structure of those complexes, we have studied the interaction between metal ions and various amino- and peptidehydroxamic acids in solution during the past 20 years. Within this time, numerous systems have been investigated in our lab and also in others by using first of all potentiometric, spectroscopic, mass spectrometric, EPR and NMR methods, and the results are discussed in reviews and regular articles [10–18].

As it is well-known, an imidazole function in the side chain of amino acids [16], small peptides [19] or protein molecules [20], is one of the most effective metal binding sites. This is the reason, why the role of the imidazole moiety at the R_C substituent of various monohydroxamic acids ($R_CC(O)N(R_N)OH$) has been intensively studied previously. First of all, metal complexation of histidinehydroxamic acid (Hisha) has been investigated [16,21–24]. In addition to the imidazole-*N* and hydroxamic function, this molecule also contains an amino-*N*, what can play crucial role in the

* Corresponding author.
E-mail addresses: efarkas@delfin.unideb.hu, efarkas@delfin.klte.hu (E. Farkas).

0277-5387/$ - see front matter © 2010 Elsevier Ltd. All rights reserved.
doi:10.1016/j.poly.2010.08.023

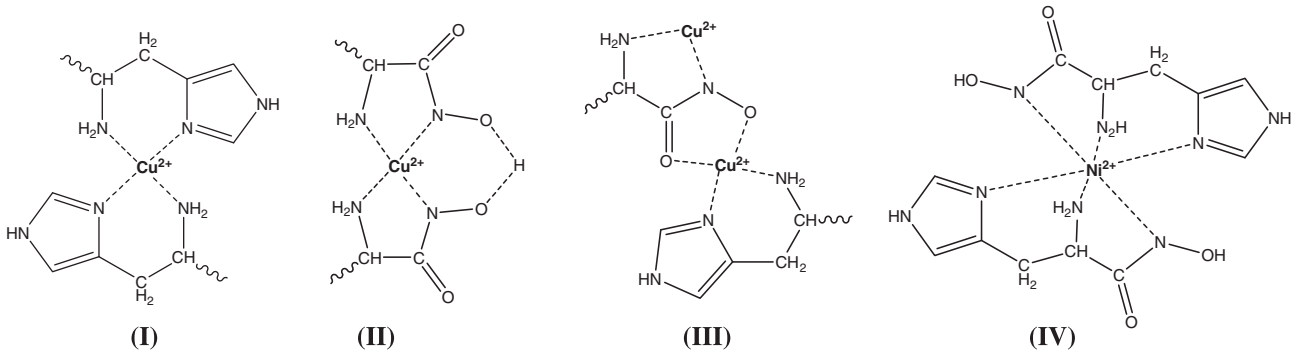

Scheme 1.

coordination. According to the results, the coordination with Cu^{2+} starts at pH ca. 3–3.5 via hydroxamate-*O* donors, but as the pH is increased, the binding via the nitrogen donors becomes more and more dominant. Between pH 4.5–7 the amino-*N* and the imidazole-*N* donors coordinate in the complexes $[CuH_2L_2]^{2+}$ and $[CuHL_2]^{+}$ (Scheme 1(**I**)). Further increase of the pH results in the formation of $[CuL_2]$, in which the hydroxamate-*N* (instead of imidazole-*N*) together with the amino-*N* coordinates the metal ion. Above pH 9, the deprotonation of one of the coordinated hydroxamates occurs and a "hydroximato" chelate appears in the complex $[CuH_{-1}L_2]^{-}$ (**II**). Within the pH-range 4–7 oligonuclear species in low concentration with mixed coordination mode (**III**) were also supported [16]. The "histamine-type" coordination mode (**I**) was found to dominate in the complexes $[NiH_2L_2]^{2+}$ and $[NiHL_2]^{+}$, while amino-*N*, imidazole-*N* and hydroxamate-*N* donors bind to the metal ion in $[NiL_2]$ (**IV**). Above pH ca. 9, parallel with the formation of $[NiH_{-1}L_2]^{-}$ the geometry of the complex changes from octahedral to square planar [16].

In the Zn^{2+}-containing systems, although different coordination isomers were found, but the preference of the hydroxamate oxygens for metal binding was evidenced. Hydroxamate-type coordination is suggested in the $[ZnHL]^{2+}$ and $[ZnH_2L_2]^{2+}$ below pH 6. Above this pH, where the ligands loose their dissociable proton, NMR results support the binding via the amino-*N*, imidazole-*N* and one of the hydroxamic-*O* donors [16].

One of the most surprising results was obtained for the complexation of this ligand with Fe^{3+}. According to one of our previous works, the formation of the well-known tris-hydroxamato-type complex is significantly hindered in the Fe^{3+}-Hisha system even at 1:10 metal to ligand ratio. On the other hand, the results indicated metal-metal coupling in the pH range, where stepwise deprotonation of the bis-complex, $[Fe(H_2L)_2]^{5+}$ started (above pH 4). Based on the findings, the involvement of the nonprotonated side chain donors (imidazole-*N* and, at higher pH the amino-*N*) in the coordination was suggested and coordinative or noncovalent interaction (e.g., H-bond between the already nonprotonated and still protonated imidazoles, or between the imidazole-*N* and ammonium-NH_3^+ protons, and/or stacking interaction) was assumed. At high pH ESI-MS supported the existence of bis-hydroxamato-monohydroxo species [16].

As a continuation of the previous study, new imidazole analogous of α-alaninehydroxamic acid, β-alaninehydroxamic acid and *N*-methyl-α-alaninehydroxamic acid have been synthesized and investigated in our lab in a recent work [25]. In this study we have found that, the presence of the strong imidazole-*N* donor in α-or β position to the hydroxamic moiety can significantly affect the metal binding capability of the molecule. The imidazole-*N* is the anchor donor not only in the case of Cu^{2+}-, and Ni^{2+}-, but even in the Zn^{2+}-containing systems. Water insoluble polynuclear complexes were formed with the α-derivative, but a pentanuclear metallocrown, $[Cu_5H_{-4}L_4]^{2+}$ exclusively exists with the β-derivative over a wide pH-range in the Cu^{2+}-containing system. Interestingly, this metallocrown was also confirmed with Ni^{2+} and Zn^{2+}, although with lower stability than with Cu^{2+} [25].

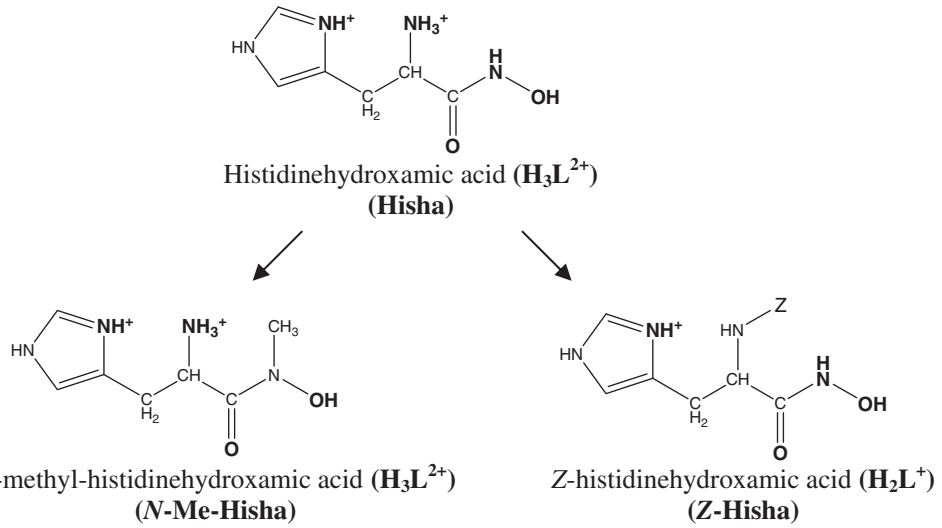

Scheme 2.

In the present work two new histidinehydroxamic acid derivatives (*N*-methyl-histidinehydroxamic acid and *Z*-histidinehydroxamic acid) have been synthesized and their metal binding capability with Cu^{2+}, Ni^{2+} and Zn^{2+} has been studied by using pH-potentiometric, UV–Vis, CD, EPR, ^{1}H NMR and ESI-MS measurements. In order to have a better comparison of the results, some reproductive measurements for the previously studied Hisha-containing systems [16,21–24] were also performed.

Both of the two new derivatives contain one donor atom less than Hisha. Namely, in the case of *N*-Me-Hisha the hydroxamate-*N* as donor is eliminated, while the coordination of the amino-*N* of *Z*-Hisha is not possible at all. The formulae of the totally protonated new ligands together with the parent Hisha are summarized in Scheme 2. (The possible coordinating donor atoms are marked with bold letters).

2. Experimental

2.1. Synthesis

All chemicals and solvents were analytical grade and were used without further purification. L-α-histidine, *N*-α-carbobenzyloxy-L-histidine, $NH_2OH{\cdot}HCl$, ethylchloroformiate and *N*-methylmorpholine were purchased from Aldrich, palladium/carbon (10%(m/m)) from Merck. Methanol was dried under N_2 using magnesium turnings and iodine, while dry tetrahydrofurane was also made under N_2 using sodium wire and benzophenone, according to the literature [26].

2.1.1. Z-L-α-Histidine methyl esther·HCl (**1**)

A solution of *N*-α-carbobenzyloxy-L-histidine (*Z*-histidine) (2.00 g, 6.92 mmol) in freshly distilled dry methanol (30 mL) was bubbled with dry hydrogen chloride gas for one hour under cooling in water-ice-bath. Solvent was evaporated in vacuo affording the pure product (**1**) as white crystals. Yield: 2.00 g, 85%. ^{1}H NMR (360 MHz, DMSO-d_6) δ: 7.96 (s, 1H, imH^2), 7.37–7.26 (m, 6H, imH^5 and $-C_6H_5$), 4.99 (s, 2H, $C_6H_5CH_2-$), 4.44 (q, 1H, –CH–), 3.63 (s, 3H, $-CH_3$), 3.07–3.01 (m, 2H, $-CH_2-$).

2.1.2. Z-L-α-Histidinehydroxamic acid·HCl (Z-Hisha) (**2**)

To a cooled solution of *Z*-L-α-histidine methyl esther·HCl **(1)** (2.00 g, 5.89 mmol) in dry MeOH (30 mL) was added a solution of KOH in MeOH (0.33 g, 5.89 mmol) under stirring. In another flask 0.74 g (10.60 mmol) $NH_2OH{\cdot}HCl$ and 0.86 g (15.32 mmol) KOH pastilles were dissolved in 30 mL MeOH at 0 °C. The mixture was stirred for 15 min in water-ice bath and KCl was filtered out. Solution of free ester was added dropwise to the solution of the free hydroxylamine. The reaction mixture was stirred at 0 °C for one hour and it was kept at 4 °C overnight. The white solid was filtered, washed with ether and dried in vacuo. The crude product was recrystallized from MeOH affording pure hydroxamic acid (**2**). Yield: 350 mg, 18% ^{1}H NMR (360 MHz, DMSO-d_6) δ: 7.61 (s, 1H, imH^2), 7.37–7.31 (m, 5H, C_6H_5), 6.83 (s, 1H, imH^5), 5.00 (s, 2H, $C_6H_5CH_2-$), 4.22 (q, 1H, –CH–), 2.97–2.90 (m, 2H, $-CH_2-$). ESI-TOF MS (*m*/*z*): 305.125 $[C_{14}H_{17}N_4O_4]^+$.

2.1.3. Z-N-methyl-O-benzyl-L-α-histidinehydroxamic acid (**3**)

To an ice-cooled solution of *N*-methyl-*O*-benzyl hydroxylamine hydrochloride (1.85 g, 10.85 mmol) in dry, freshly distilled MeOH (10 mL) was added a solution of KOH (0.60 g, 10.70 mmol) in MeOH (5 mL) and the mixture was stirred for 25 min in ice-water bath under N_2. KCl was filtered and the solution was kept at 0 °C. To a chilled solution of *Z*-histidine (2.06 g, 7.13 mmol) in dry, freshly distilled tetrahydrofurane (50 mL) was added ethylchloroformiate (0.82 mL, 8.56 mmol) and *N*-methylmorpholine (1.02 mL, 9.27 mmol). After 40 min of stirring at 0 °C the solid was filtered and the solution was added dropwise to the previously prepared solution of the free hydroxylamine. The reaction mixture was stirred under N_2 in ice bath for 2 h and for further 2 h at ambient temperature. The solvent was evaporated and the oil obtained was purified by column chromatography (Kieselgel 60, eluent: $CHCl_3$:MeOH = 95:5, R_f = 0.20) Yield: 550 mg, 20%. ^{1}H NMR (360 MHz, DMSO-d_6) δ: 8.01 (s, 1H, imH^2), 7.73–7.32 (m, 11H, $-C_6H_5$, –NH), 6.95 (s, 1H, imH^5), 5.00–4.93 (m, 5H, $C_6H_5CH_2-$ and –CH–), 3.15 (s, 3H, $-CH_3$), 2.89–2.77 (m, 2H, $-CH_2-$).

2.1.4. N-methyl-L-α-Histidinehydroxamic acid·2HCl (N-Me-Hisha)(**4**)

Z-*N*-methyl-*O*-benzyl-L-α-histidinehydroxamic acid **(3)** (150 mg, 0.37 mmol) was subjected to hydrogenolysis in methanol (20 mL), using palladium charcoal (35 mg, 10% Pd) and 4–5 drops concentrated (36% (m/m)) HCl solution for four hours. After filtration and evaporation a pale yellow oil was remained. After drying in high vacuum, and treatment with ether to remove vestigiary amounts of water afforded 80 mg (90%) white crystals as the pure compound (**4**). ^{1}H NMR (360 MHz, D_2O) δ: 8.55 (s, 1H, imH^2), 7.35 (s, 1H, imH^5), 4.45 (q, 1H, –CH–), 3.45 (s, 3H, $-CH_3$), 3.06–3.02 (m, 2H, $-CH_2-$). ESI-TOF MS, *m*/*z*:: 185.102 $[C_7H_{13}N_4O_2]^+$.

2.2. Equilibrium measurements

2.2.1. Metal ion and ligand stock solutions

The purity of the ligands and the concentrations of the ligand stock solutions were determined by Gran's method [27]. The Cu^{2+} and Ni^{2+} stock solutions were prepared from $CuCl_2{\cdot}2H_2O$ and $NiCl_2{\cdot}6H_2O$ (Reanal) dissolved in bi-distilled water. ZnO (Reanal) was dissolved in a known amount of HCl solution (0.10 M). The concentration of the metal ion stock solutions was determined gravimetrically via precipitation of quinolin-8-olates [28]. The HCl concentration of the Zn^{2+} solution and the exact concentration of the carbonate-free KOH titrant were determined by pH-potentiometry.

2.2.2. Potentiometric and spectroscopic studies

The pH-potentiometric and spectrophotometric measurements were carried out at an ionic strength of 0.2 M (KCl). Temperature was 25.0 ± 0.1 °C. Carbonate-free KOH solution of known concentration (0.2 M) was used as titrant. HCl stock solution was prepared from conc. HCl. The concentration of the HCl solution was also determined by pH-potentiometric titrations using the Gran's method [27]. For *N*-Me-Hisha both pH-potentiometric and spectroscopic measurements were made in aqueous solution. Radiometer pHM 84 instrument equipped with Metrohm combined electrode (type 6.0234.100) was used for pH-potentiometric measurements with a Metrohm 715 Dosimat automatic burette. The electrode system was calibrated according to Irving et al. [29] and the pH-metric readings could, therefore be converted into hydrogen concentration. The water ionization constant (pK_w) is 13.76 ± 0.01 in aqueous solution under the conditions employed. Due to solubility problems of the complexes of *Z*-Hisha all the measurements were performed in DMSO/water 50:50% (m/m) mixture. For comparison, the previously already studied [25] Imidazole-4-carbohydroxamic acid (im-4-Cha), because its complexes show similar solubility problems, was also investigated in the present work in DMSO-water 50:50% (m/m) solvent mixture. In these cases the solvent mixture was also used for the preparation of KCl and HCl stock solutions and for the KOH titrant. The electrode was conditioned in DMSO/water 50:50% (m/m) for 3–4 days before the measurements. For the calibration of the electrode system aqueous potassium hydrogen ftalate solution was used as it is recommended by IUPAC [30]. The water ionization constant (pK_w) was found to be 15.41 ± 0.01 at these conditions.

All the pH-potentiometric titrations were performed over the pH-range of 2–11 or until precipitation occurred. Initial volume of the samples was 4.00 or 5.00 mL. Ligand concentration was 2–3×10^{-3} M and the metal to ligand ratios were 1:1, 1:2 and 1:3, 1:4 or 1:5. During the titrations purified, strictly oxygen-free argon was continuously bubbled through the samples. The pH-metric results were utilized to find the stoichiometry of species and to calculate the stability constants. The calculations were made with the aid of the computer program PSEQUAD [31].

UV–Vis measurements on systems containing Cu^{2+} and Ni^{2+} were performed. In the case of Cu^{2+}-containing systems ligand concentrations were varied within the range 2.2–2.8×10^{-3} M and the Cu^{2+} to ligand ratios were 1:1 and 1:2 for both ligands. For Ni^{2+}-containing systems the concentration of the *N*-Me-Hisha was 1.2×10^{-2} M and the metal to ligand ratios were 1:2 and 1:4. A Perkin–Elmer Lambda 25 spectrophotometer was used to record the spectra in the region of 290–900 nm. Path length was 1 cm in all cases.

CD spectra for Cu^{2+}-*N*-Me-Hisha samples at 1:1 and 1:2 metal to ligand ratios were also obtained at 25 °C under a constant flow of nitrogen on a Jasco J-810 spectropolarimeter, which was calibrated with an aqueous solution of the ammonium salt of (1R)-(-)-10-camphorsulfonate. The ligand concentration in the samples was 2.5×10^{-3} M. Measurements were carried out in aqueous solution at different pH values, using 1 cm path length cuvettes in the 290–800 nm wavelength regions.

^{1}H NMR spectra were recorded for *N*-Me-Hisha and *Z*-Hisha and for their Zn^{2+}complexes on a Bruker Avance AM 360 by using D_2O or $(CD_3)_2SO$ as solvent and DSS ((2,2-dimethyl-2-silapentane-5-sulfonic acid, sodium salt) as standard under the following conditions: metal to ligand ratio was 1:2 in all samples and the analytical concentration was 5×10^{-3} M for both ligands. 0.1 M NaOD and DCl solutions were used to adjust the appropriate pD.

EPR spectra of frozen aqueous solutions of the Cu^{2+}-*N*-Me-Hisha systems were recorded at 77 K at different pH values, using a Bruker EleXsys X-band spectrometer. (Parameters: microwave frequency: 9.81 GHz, modulation amplitude: 5G, modulation frequency: 100.0 kHz, microwave power: 12 mW) Methanol was added to the samples to avoid the crystallization of the water. The concentration of the Cu^{2+} was 2×10^{-3} M in all samples. The spectra were recorded at five different pH values within the pH-range 2–7 at ca. 1:1 metal to ligand ratio, while eleven spectra were registered in the pH-range 2–9 at 1:5 ratio. For the calculation of the spectra, "EPR program" was used [32]. Decomposition of the measured spectra were done by fitting the anisotropic EPR parameters ($g_{||}$, $g\perp$, copper hyperfine couplings $A_{||}$, $A\perp$, and nitrogen superhyperfine couplings a_N), the orientation dependent linewidth parameters, and the concentration ratio of the components. Since the copper(II) used in the solutions was a natural mixture of the isotopes, the spectrum of each species was calculated as the sum of spectra containing ^{63}Cu and ^{65}Cu in their natural abundances.

To obtain additional support for the complexes formed in the Cu^{2+}-*Z*-Hisha and Cu^{2+}-*N*-Me-Hisha systems electro-spray ionization time-of-flight mass spectrometric (*ESI-TOF MS*) analysis was carried out on a Bruker BIOTOF II ESI-TOF instrument. The metal to ligand ratio was 1:1 in both cases. The pH of the Cu^{2+}-*Z*-Hisha sample was 4.50, the concentration of the ligand was 5×10^{-4} M. For the other system the applied ligand concentration was 1×10^{-3} M and the spectrum was recorded at pH 5.30. The solutions were introduced directly into the ESI source by a syringe pump (Cole-Parmer Ins. Comp. type 74900) at a flow rate of 2 μL/min. The temperature of drying gas (N_2) was 100 °C. The pressure of the nebulizating gas (N_2) was 30 psi. Voltages applied at the capillary entrance, capillary exit and the first and the second skimmers were −4500, 120, 40 and 30 V, respectively. The spectra were accumulated and recorded by a digitalizer at a sampling rate of 2 GHz. The spectrometer was operated at unit mass resolution and was calibrated to sodium trifluoroacetate.

3. Results and discussion

3.1. Acidity of the ligands

Similarly to Hisha, *N*-Me-Hisha involves three dissociable protons in its totally protonated form (H_3L^{2+}), one at the terminal amino-*N*, another one at the hydroxamic function, while the third one at the side chain imidazole-*N*. Due to the presence of the *Z*-protecting group, *Z*-Hisha can liberate only two protons, one from the hydroxamic moiety while the other from the imidazole-*N*. The overall stability constants ($\log \beta$) of the two new ligands and Hisha have been determined by pH-potentiometry, and together with the stepwise dissociation constants (pK_a) calculated from the overall values are summarized in Table 1.

The dissociation constants obtained in the present work for the Hisha are in good agreement with the previously published ones [16]. As it is known from the literature, the three dissociation processes of this ligand overlap significantly [16,33]. As a consequence, the values in Table 1 are macroconstants and can not be ascribed unambiguously to the individual groups. Although great effort has been previously made by NMR for determination of the dissociation microconstants of Hisha, but because of the significant electronic effect of each group on the dissociation of the others, the microconstants could not be obtained, therefore, only trends for the acidity were suggested. Namely, the imidazolium moiety is the most acidic, while the acidity of the other two groups is close to each other [16,33]. In this latter issue the NH_3^+ group was found a bit more acidic than the CONHOH function in simple α-aminohydroxamic acids [16,34].

If a comparison of the values of *N*-Me-Hisha with those of Hisha is made, the following conclusion can be drawn: (i) The pK_{a1} values, which in high extent, belong to the deprotonation of the imidazolium group, are similar in both molecules. (ii) The difference between the second and third dissociation macroconstants of *N*-Me-Hisha is less than that of Hisha. This might be attributed to the lack of possibility for hydrogen bonding in *N*-Me-Hisha, which can be expected between the hydroxamic-NH and amino-NH_2 in Hisha. Moreover, the methyl-substituent on the hydroxamic-*N* slightly decreases the basicity of the hydroxamate group of *N*-Me-Hisha as compared to the Hisha[1] [16].

Due to the solubility problem of the metal complexes of *Z*-Hisha the stability constants of these species could not be determined in aqueous solution, therefore DMSO-water 50:50% (m/m) solvent mixture was applied. As a consequence, to calculate the stability constants of the metal complexes, determination of the dissociation macroconstants of *Z*-Hisha not only in water but also in the solvent mixture was necessary. If the corresponding pK_a values determined in the two solvents are compared with each other, one can see that the pK_{a1} (which belongs to the deprotonation of the imidazolium-NH^+) is lower, but the pK_{a2} (belongs to the hydroxamic function) is higher in DMSO-water mixture. This observation is in good agreement with earlier findings in the literature [36]. Namely, the deprotonation of the positively charged imidazolium-NH^+ yielding neutral moiety is more favoured in the less polar DMSO-water mixture than in aqueous solution, while the deprotonation of the neutral hydroxamic function, resulting in negatively charged species, is less favoured in the solvent mixture.

[1] This is the case, because the electron density donating ability of the methyl group increases the delocalization of the lone pair electrons of N via the C–N bond. This effect allows positive charge density to build up on the N atom and thereby stabilizes the conjugate base anion by induction [35].

Table 1
Overall stability constants (log β) and the stepwise dissociation constants (pK_a) of Hisha, *N*-Me-Hisha and *Z*-Hisha, t = 25.0 °C, I = 0.20 M (KCl).[a]

Ligand	Solvent		$[H_3L]^{2+}$	$[H_{2L}]^{+}$	[HL]
Hisha	water	log β	21.47(1)	16.12(1)	9.03(1)
		pK_a	5.35	7.09	9.03
N-Me-Hisha	water	log β	21.70(1)	16.31(1)	8.94(1)
			5.39	7.37	8.94
Z-Hisha	water	log β		15.22(1)	8.80(1)
		pK_a		6.42	8.80
	DMSO-water	log β		15.43(1)	9.81(1)
	50:50% (m/m)	pK_a		5.62	9.81

[a] Numbers in parentheses indicate standard deviations.

3.2. Metal complexes

3.2.1. Cu^{2+}-, Ni^{2+}- and Zn^{2+}-complexes of N-Me-Hisha

As a result of the methylation of the hydroxamate-*N* in the *N*-Me-Hisha this ligand contains two separated chelating groups, which are not able to coordinate to the same metal ion at the same time. One chelate can be formed via the hydroxamate oxygens ([O,O]- coordination) and another one via the amino-*N* and imidazole-*N* donors ([NH_2,N_{imid}]-chelate). To determine the stoichiometry and stability constants of the metal complexes, pH-potentiometric titrations were performed. Representative titration curves recorded for the *N*-Me-Hisha and for the Cu^{2+}-, Ni^{2+}- and Zn^{2+}-containing systems at 1:1 metal to ligand ratio are shown in Fig. 1.

As it is well demonstrated in Fig. 1 the ligand starts to interact with Cu^{2+} below pH = 3, with Ni^{2+} at only pH ~4, while the complexation with Zn^{2+} starts above pH ~5. Precipitation occurs in the Cu^{2+}-containing system (**1**) above pH ~5, while it occurs at pH ca. 10 or pH ~8 if the metal ion is Ni^{2+} (**2**) and Zn^{2+} (**3**), respectively. Under conditions of 1:2 metal to ligand ratio (curves not shown here) precipitation does not occur in the Cu^{2+} and Ni^{2+} -containing systems, which indicate some interactions with ligand excess.

Stoichiometry of the complexes and the overall stability constants yielding the best fit of the pH-metric titration curves are shown in Table 2.

Table 2 shows the formation of numerous protonated mono- and bis-complexes and the formation of tris-complexes is also detected in the Ni^{2+}-containing system. With Cu^{2+}, similar fitting was obtained with two models. The first included a monomeric $[CuL]^{+}$ instead of the dimeric $[Cu_2L_2]^{2+}$ which was involved in the second one. (Fitting parameters were: 3.9 and 3.8×10^{-3} cm^3, respectively). Because pH-potentiometry could not differentiate between these two species, ESI-MS measurement was used to solve this problem. The result obtained for aqueous solution at pH 5.3 unambiguously showed the existence of $[Cu_2L_2]^{2+}$ in this system

Table 2
Overall stability constants (log β_{pqr}) for the Cu^{2}+-, Ni^{2}+- and Zn^{2}+-complexes formed with *N*-Me-Hisha, t = 25.0 °C, I = 0.20 M (KCl).[b]

	Complex	p	q	r	log β_{pqr}		
					Cu^{2+}	Ni^{2+}	Zn^{2+}
N-Me-Hisha	$[MH_2L]^{3+}$	1	2	1	20.2(1)		
	$[MHL]^{2+}$	1	1	1	17.46(2)	15.45(2)	13.52(3)
	$[ML]^{+}$	1	0	1		9.09(3)	6.97(3)
	$[MH_{-1}L]$	1	−1	1			−1.37(4)
	$[M_2L_2]$	2	0	2	29.52(3)		
	$[MH_2L_2]^{2+}$	1	2	2	32.61(9)	29.69(4)	26.86(4)
	$[MHL_2]^{+}$	1	1	2	25.5(1)	22.69(7)	19.70(6)
	$[ML_2]$	1	0	2	17.45(7)	14.53(9)	11.51(7)
	$[MHL_3]$	1	1	3		26.9(2)	
	$[ML_3]^{-}$	1	0	3		18.4(2)	
	Number of experimental points				220	150	90
	Fitting parameter (cm^3)				0.0038	0.0028	0.0021

[b] Numbers in parentheses indicate standard deviations.

($[Cu_2L_2]^{2+}$ = 247 m/z, $[Cu_2L_2]Cl^{+}$ = 529 m/z), therefore the equilibrium model involving the dimeric complex was finally accepted.

In order to determine the most probable binding modes of the complexes, UV–Vis, CD and EPR measurements have been performed.

Out of the results, representative concentration distribution curves calculated at 1:2 metal to ligand ratio, together with the λ_{max} values of the visible spectra as a function of pH are presented in Fig. 2.

By the decomposition of the registered EPR spectra, individual spectra (Fig. 3) could be calculated for the mononuclear complexes formed in this system. As it is demonstrated in Fig. 2, at pH ca. 2.5 the free Cu^{2+} dominates, which was also supported by the EPR results (S1 shows the measured EPR spectra together with simulated curves). The first measurable (but not dominant) complex is $[CuH_2L]^{3+}$. Out of the two possible coordination modes in this species (monodentate coordination of imidazole-*N* or hydroxamate-[O,O]-chelation) the former seems more probable by the EPR parameters ($A_{||}$ = 139.6 × 10^{-4} cm^{-1} and $g_{||}$ = 2.373) [37]. This is further supported by lack of the charge-transfer band at λ_{max} = 380 nm, which would be characteristic for the involvement of the hydroxamate-*O* in the coordination below pH ~3 [14,38].

Upon increasing the pH, $[CuHL]^{2+}$ is formed and the EPR results clearly indicate the existence of two different isomers of this complex. The hydroxamate-*O* donors coordinate to the metal ion in one of the isomers (the $A_{||}$ = 166.8 × 10^{-4} cm^{-1} and $g_{||}$ = 2.305 parameters are similar to those previously published for [O,O] coordination [39] and also the characteristic charge-transfer band in the

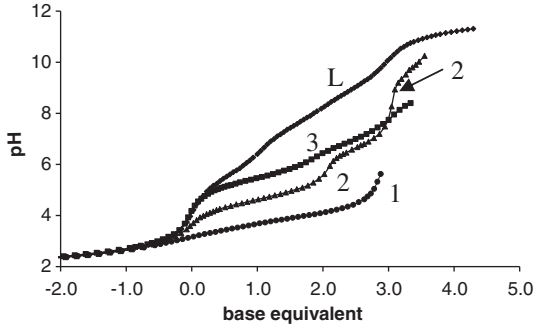

Fig. 1. Representative pH-potentiometric titration curves registered for *N*-Me-Hisha (**L**) and for Cu^{2+}-(**1**), Ni^{2+}-(**2**), Zn^{2+}-(**3**) *N*-Me-Hisha systems at 1:1 metal to ligand ratio, c_L = 2.6 × 10^{-3} M.

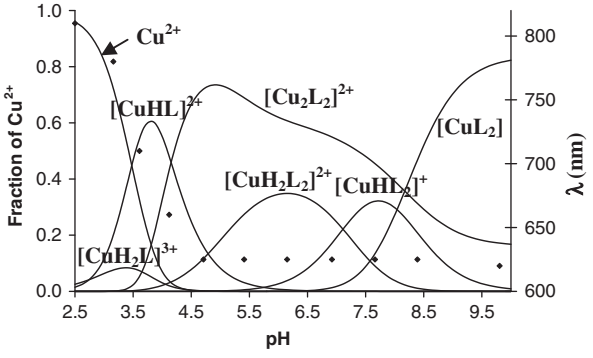

Fig. 2. Representative concentration distribution curves calculated for Cu^{2+}-*N*-Me-Hisha system at 1:2 metal to ligand ratio, together with the λ_{max} values of the d–d band, c_L = 2.5 × 10^{-3} M.

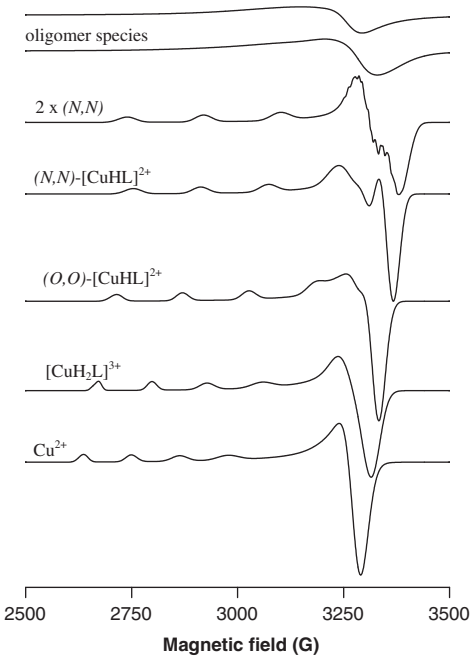

Fig. 3. Simulated component EPR spectra of some of the complexes formed in the Cu^{2+}-*N*-Me-Hisha system.

UV–Vis spectrum appears), while the greater linewidth of the parallel lines and the stronger ligand field ($A_{||} = 165.5 \times 10^{-4}$ cm^{-1} and $g_{||} = 2.272$) support the formation of the [NH_2,N_{imid}]-chelate in the other isomer. Based on the EPR results at 1:1 metal to ligand ratio, it was possible to make an estimation for the ratio of these isomers and 60:40% was calculated for the ratio of the *(O,O)*-$[CuHL]^{2+}$ to the histamine-type *(N,N)*-$[CuHL]^{2+}$.

Regardless of the metal to ligand ratio the minimum λ_{max} of the registered d–d band is at 625 nm in this system. This is demonstrated e.g. in Fig. 2, where the λ_{max} does not show any change above pH 4.5, but remains at the above mentioned 625 nm. Taking into account that the λ_{max} is 650 nm for the bis(acetohydroxamato-*O,O*)copper complex [38], while 600 nm for the bis(histamine-*N,N*)copper [40] and by using the Sigel–Martin's equation [41], the λ_{max} = 625 nm strongly supports the presence of two hydroxamate oxygens, plus one amino-nitrogen and one imidazole-nitrogen per Cu^{2+} in the coordination sphere of all the complexes ($[Cu_2L_2]^{2+}$, $[CuH_2L_2]^{2+}$, $[CuHL_2]^{+}$, $[CuL_2]$) formed above pH 4.5 in the Cu^{2+}-*N*-Me-Hisha system. Similarly, the CD parameters also indicate the presence of these types of chelates by the two bands at λ_{max} = 380 nm(+) and 680 nm(+)) at pH ca. 4. (The band at λ_{max} = 380 nm indicates the involvement of the hydroxamate-*O* in the coordination [15], while the positive Cotton-effect at 674 nm can be assigned to the histamine-type coordination [42].) As the pH is further increased, any change in the CD spectrum, except some increase in the intensity of the bands does not occur. The spectroscopic results detailed above support the parallel coordination of the hydroxamate-type [O,O] and histamine-type [NH_2,N_{imid}] chelates of *N*-Me-Hisha. However, in a 1:1 metal to ligand complex this is not possible in monomeric species. This assumption is supported by the existence of species with a broad singlet EPR line in the system above pH 3.5 and fits to the formation of the dimeric complex $[Cu_2L_2]^{2+}$, in which the line broadening can be explained by the dipole–dipole coupling between the two paramagnetic centers. The amount of this complex is dominant even at ligand excess (see Fig. 2). The predominance of this mixed coordination mode ([O,O]- and [NH_2,N_{imid}]-chelates) is also supported in the bis-complexes ($[CuH_2L_2]^{2+}$, $[CuHL_2]^{+}$, $[CuL_2]$) both by the UV–Vis and EPR results, but the EPR spectra registered at 1:5 metal to ligand ratio also indicate the formation of bis-complex(es) with 4N donors (two [NH_2, N_{imid}]-chelates in low concentration. The well resolved superhyperfine structure of the EPR spectra could be well described by taking into account two pairs of equivalent nitrogens and the rhombic symmetry of g- and A-tensors for this complex ($g_{xx} = 2.043$, $g_{yy} = 2.055$, $g_{zz} = 2.259$, $A_{xx} = 13.7 \times 10^{-4}$ cm^{-1}, $A_{yy} = 8.6 \times 10^{-4}$ cm^{-1}, $A_{zz} = 186.1 \times 10^{-4}$ cm^{-1}, $a_{Nxx} = 8 \times 10^{-4}$ cm^{-1} (13×10^{-4} cm^{-1}), $a_{Nyy} = 14 \times 10^{-4}$ cm^{-1} (9×10^{-4} cm^{-1}) $a_{Nzz} = 10 \times 10^{-4}$ cm^{-1} (6×10^{-4} cm^{-1})). Although *cis* or *trans* arrangement of the two [NH_2, N_{imid}] chelates in this bis-complex cannot be determined from the EPR parameters, the sharp perpendicular lines (well resolved nitrogen splitting) and the steric hindrance of the two imidazole ring in the *cis* arrangement make the predominance of the *trans* isomer more probable (structure (**I**) in Scheme 1).

In the case of Ni^{2+} the first buffer region in Fig. 1 shows that two protons of the ligand are liberated by this metal ion in one step (below pH ~4.5), while the third dissociable proton is released in a separated process in the pH-range 6.0–8.0, where the deprotonation of a non-coordinated hydroxamic function can occur. Taking these findings into account, one can conclude that the first buffer region most probably belongs to the deprotonation and coordination of the amino-*N* and imidazole-*N*, while the hydroxamate moiety is still protonated. The separated second base-consuming region most probably belongs to the deprotonation of the non-coordinated hydroxamic function. Due to the formation of bis- and tris-complexes, ligand excess is able to hinder the hydrolysis of the metal ion. Representative concentration distribution curves calculated at 1:4 metal to ligand ratio, demonstrate the high preference of the bis- and tris-complexes in this system (Fig. 4). This figure also shows the λ_{max} values belonging to the $^3A_2 \rightarrow {}^3T_1$ (F) transition in the visible spectra.

There is no indication for the formation of square planar complexes in the Ni^{2+}-*N*-Me-Hisha system, only octahedral complexes exist in the pH-range 3–10. The coordination of the amino-*N* and imidazole-*N* is unambiguously supported by the UV–Vis results (see Fig. 4, where the λ_{max} ($^3A_2 \rightarrow {}^3T_1$ (F)) is at 550 nm, ε ~50 mol^{-1} dm^3 cm^{-1} at pH ~7.0 and parallel with the formation of tris-complexes above pH ~7.5, it decreases to 542 nm, ε ~48 mol^{-1} dm^3 cm^{-1}). Hydroxamate-[O,O] coordination would result in significantly higher λ_{max} values. (The corresponding λ_{max} for the bis-[NH_2,N_{imid}]-chelated complex of Ni^{2+}-histamine is at 570 nm [40], while it is at 649 nm for the bis(acetohydroxamato-*O,O*)nickel complex [38]). As a conclusion, it can be suggested that histamine-like coordination mode predominates in the Ni^{2+}-*N*-Me-Hisha complexes and there is no indication for the coordination of the hydroxamate-oxygens. The proposed structure of the $[NiL_3]^-$ is presented in Scheme 3.

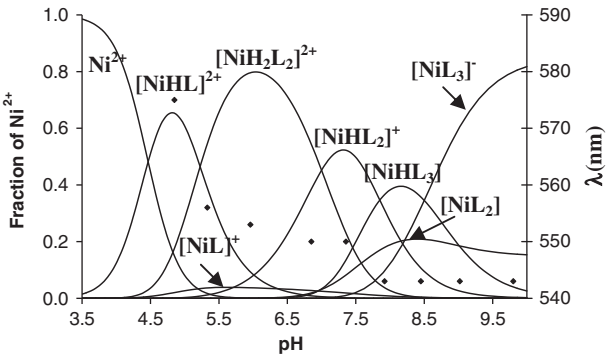

Fig. 4. Concentration distribution curves calculated for Ni^{2+}-*N*-Me-Hisha system at 1:4 metal to ligand ratio together with the λ_{max} values of the d–d band, $c_L = 2.6 \times 10^{-3}$ M.

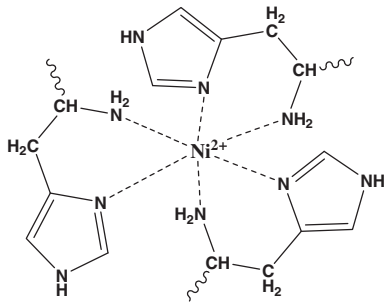

Scheme 3.

As Fig. 1 also indicates, this ligand starts to interact with Zn^{2+} above pH ~5.0 and precipitation occurs above pH ~8. Therefore the pH-metric titration curves could be fitted in a relatively narrow pH range. In contrast to the Ni^{2+}-containing system, the three equivalents base consumption does not occur in separated steps in the case of Zn^{2+}. The deprotonation of the ligand and the hydrolysis of the metal ion take place in overlapping processes. In addition to the pH-potentiometric measurements ^1H NMR technique has also been applied to investigate the interaction between the ligand and the diamagnetic Zn^{2+} ion.

The chemical shifts of the C(2)H and C(5)H protons of the imidazole are assumed to be sensitive to the metal ion coordination via imidazole-*N(3)*, while the *N*-methyl protons are expected to feel the coordination of the hydroxamate function. In good agreement with the pH-potentiometric titration, measurable interaction between the ligand and the metal ion was indicated by the NMR results above pH ~5. It was also found that both the imidazole- and methyl-protons showed similar changes (~0.05–0.06 ppm) in the chemical shifts in the Zn^{2+}-containing system compared to the free ligand. This may suggest that neither the hydroxamate-[O,O], nor the histamine-type [NH_2,N_{imid}]-chelates play a major role in the Zn^{2+} binding, therefore the formation of different linkage isomers occurs in the Zn^{2+}-*N*-Me-Hisha system.

3.2.2. Cu^{2+}-, Ni^{2+}- and Zn^{2+}-complexes of Z-Hisha

Due to the very poor water solubility of the complexes formed with this ligand all the measurements were carried out in DMSO-water 50:50% (m/m) solvent mixture. Representative pH-metric titration curves of Cu^{2+}-, Ni^{2+}- and Zn^{2+} -*Z*-Hisha systems at 1:1 metal to ligand ratio are shown in Fig 5.

As Fig. 5 clearly shows, there are significant differences in the pH effects, which obviously indicate great differences in binding ability of this ligand towards Cu^{2+} compared to those with Ni^{2+} or Zn^{2+}. While very strong interaction is suggested in the case of Cu^{2+}, the titration curves show only weak interaction with Ni^{2+} and Zn^{2+}. The equilibrium models yielding the best fit of the pH-metric experimental data and the calculated stability constants are summarized in Table 3.

Representative concentration distribution curves calculated for the Cu^{2+}-*Z*-Hisha system at 1:1 metal to ligand ratio together with the λ_{max} values of the d–d band are presented in Fig. 6. As Fig. 6 shows, the complexation starts above pH ~2.5 and the stoichiometry of the first complex formed is $[CuHL]^{2+}$ (see also Table 3). In this species, the hydroxamic function is still protonated and monodentate-N_{imid} coordination mode is suggested. The charge-transfer band at 380 nm, which is characteristic for the Cu^{2+}-hydroxamate interaction, appears only above pH 3.3 parallel with the formation of the species $[CuL]^+$ and the polynuclear complex, $[Cu_5H_{-4}L_4]^{2+}$.

$[CuL]^+$ is a minor complex in this system, existing in a narrow pH-range and in a maximum of ca. 17% at 1:1 metal to ligand ratio (Fig. 6). Because the stability constant associated with this species is really high (even if the solvent effect is taken into account), most probably both the hydroxamate moiety and the imidazole-*N* are involved in the coordination. However, the simultaneous coordination of these donors (what would be resulted in formation of a seven-membered chelate joined to a five-membered one) can not be favoured in monomeric species, therefore the formulae of $[CuL]^+$ might be given as $[CuL]_x^{x+}$.

As the pH is increased above pH 3.5 the formation of a very stable pentanuclear complex starts. Both the ESI-MS result (Fig. 7) obtained at pH 4.3 and fitting of the pH-potentiometric data (Fig. 5) support predominance of the species $[Cu_5H_{-4}L_4]^{2+}$ (m/z = 763).

The structure of the suggested 12-metallacrown-4 (12-MC-4)-type complex is shown in Scheme 4. Interestingly, as it can be seen in this Scheme, 7-membered [N_{imid}, N_{hydr}]-and 5-membered [O,O]-chelates are involved in this polynuclear species.

As it is well-known from previous results, extremely stable 12-MC-4 type copper(II) complexes involving 6-membered [N_{amino}, N_{hydr}]- and 5-membered [O,O]-chelates are predominant over a wide pH-range with β-aminohydroxamates. If the ligand is

Table 3
Overall stability constants (log β_{pqr}) for the Cu^{2+}-, Ni^{2+}- and Zn^{2+}-complexes formed with *Z*-Hisha in DMSO-water 50:50 % (m/m), t = 25.0 °C, I = 0.20 M (KCl).[c]

Ligand	Complex	p	q	r	log β_{pqr}		
	Zn				Cu^{2+}	Ni^{2+}	Zn^{2+}
Z-Hisha	$[MHL]^{2+}$	1	1	1	14.31(8)	13.02(7)	13.00(3)
	$[ML]^+$	1	0	1	10.40(6)	6.81(3)	6.61(3)
	$[M_5H_{-4}L_4]^{2+}$	5	−4	4	38.5(2)		
	Number of experimental points				90	70	80
	Fitting parameter (cm^3)				0.0034	0.003	0.0022

[c] Numbers in parentheses indicate standard deviations.

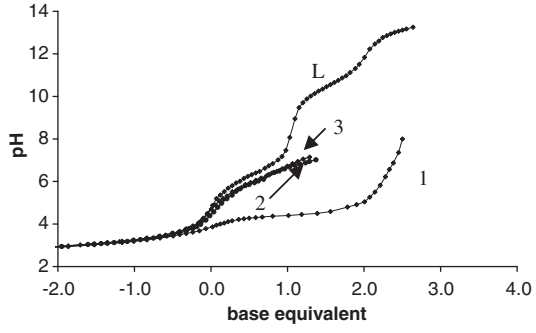

Fig. 5. Representative pH-potentiometric titration curves registered for *Z*-Hisha (**L**) and for Cu^{2+}-(**1**), Ni^{2+}-(**2**), and Zn^{2+}-(**3**) *Z*-Hisha systems at 1:1 metal to ligand ratio in DMSO-water 50:50% (m/m) solvent mixture, $c_L = 2.3 \times 10^{-3}$ M.

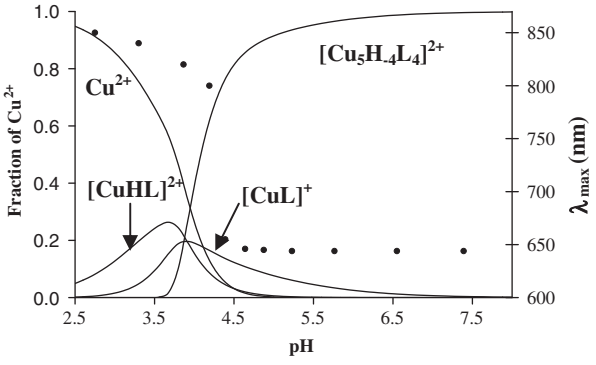

Fig. 6. Representative concentration distribution curves registered for Cu^{2+}-*Z*-Hisha system at 1:1 metal to ligand ratio together with the λ_{max} values of the d–d band, $c_L = 2.3 \times 10^{-3}$ M.

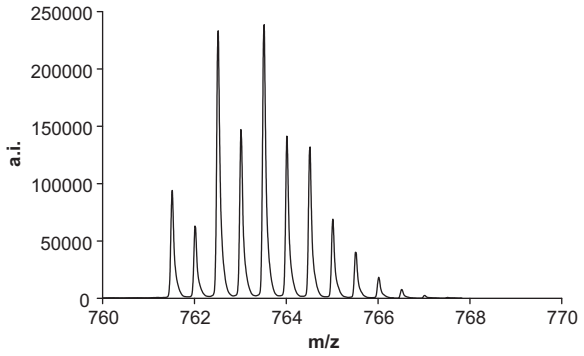

Fig. 7. ESI-MS spectrum registered for Cu^{2+}-*Z*-Hisha system at pH 4.3 at 1:1 ratio, $c_L = 1 \times 10^{-4}$ M.

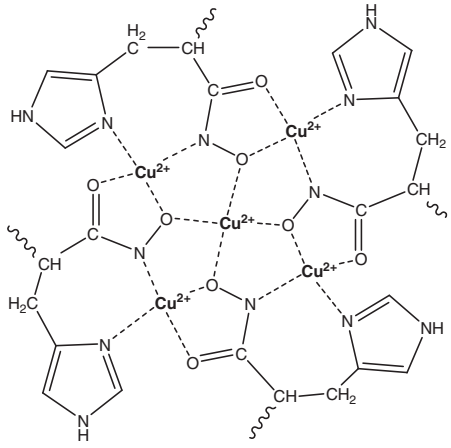

Scheme 4.

an α-aminohydroxamate, the formation of the 12-MC-4 is restricted to an intermediate pH-range, ca. 4-6, because the conditional stability of the 4N-coordinated species, *bis*(α-aminohydroxamate-N_{amino},N_{hydr})copper, becomes higher compared to that of the metallacrown above pH 6 [10–12,16]. The formation of a 12-MC-4 type complex with two γ-aminohydroxamic derivatives, (*S*)-glutamic-γ-hydroxamic acid and γ-aminobutanehydroxamic acid, was found only recently and the stability of these metallacrowns are lower than the corresponding ones with α-, or β-derivatives [10].

Recently, we were able to confirm the formation of a 12-MC-4 type complex also with α- and β-imidazole analoges [25] and now, the results presented here in this paper clearly support the existence of metallacrown with the γ-imidazole-hydroxamic acid derivative, *Z*-Hisha. If the stability constants (log β) obtained for the $[Cu_5H_{-4}L_4]^{2+}$ formed with α-, β- and γ-derivatives (Imidazole-4-carbohydroxamic acid, Imidazole-4-acetohydroxamic acid and *Z*-Hisha) are compared, the values of 44.11[2], 46.32 [25] and 38.5 (see Table 3), respectively, can be obtained. Especially, if it is taken into account that the constant for the β-derivative was determined in pure water, while the two others in DMSO-water mixture, the same stability order (β > >α > γ) can be seen as it was published with aminohydroxamic acids [10]. Even if the value related to the metallacrown with *Z*-Hisha is the lowest in this series (triad), it is still high enough to hinder the hydrolysis of the Cu^{2+} below pH 9.

In contrast to Cu^{2+}, the other two investigated metal ions show only weak interaction with *Z*-Hisha (Fig. 6). The titration curves could be fitted only in a narrow pH range, because the complexation starts at ca. pH 4 and above pH 6 precipitate occurred. Only the formation of $[MHL]^{2+}$ and $[ML]^{+}$ was found. With Ni^{2+} the titration curve indicates weak imidazole-*N* coordination, while in the case of Zn^{2+}, based on the previous results with Hisha, the complex formation with the hydroxamate-*O* is likely. Weak interaction can also be seen with the presence of the imidazole-*N* (Fig. 6), but the chemical shifts of the C(2)H and C(5)H protons of the ligand show negligible interaction of the metal ion with the imidazole moiety in the NMR measurements.

4. Conclusion

Elimination of hydroxamate-*N* as a donor atom by its methylation provides a typical ambidentate character for the *N*-Me-Hisha. The role of the two (practically independent) chelating functions, histamine-type [NH_2,N_{imid}]-chelate and hydroxamate-type [O,O]-chelate, in the coordination highly depends on the metal ion.

N-Me-Hisha behaves towards Ni^{2+} ion as a histamine derivative, the interaction starts at pH ~4 and histamine-type chelates predominate in the nickel-complexes.

There is no significant difference between the conditional stability of a histamine-type and a hydroxamate-type chelate if the metal ion is Cu^{2+}, and also the pH-range of their formation overlaps significantly. Both types of chelates have high stability, start to form with Cu^{2+} at pH ~3 and the mixed-type bis-chelated coordination mode is the most favoured in this system. This is resulted in favoured formation of $[Cu_2L_2]^{2+}$, in which the two chelates of each ligand are coordinated to different metal ions, and also the coordination mode is mixed-type in the bis-complexes formed in presence of excess of the ligand.

Because neither the hydroxamate-[O,O]-, nor the histamine-type [NH_2,N_{imid}]-chelates play a major role in the Zn^{2+} binding, the formation of different low stability mono-chelated linkage isomers occurs in the Zn^{2+}-*N*-Me-Hisha system above pH 5.

In spite of the well-known very high affinity of a hydroxamate chelate towards the Fe^{3+} ion, surprisingly, histamine-type chelate was found to have some role in the complexes formed in the Fe^{3+}-*N*-Me-Hisha in a recent work in our laboratory [43].

The protecting of the terminal amino moiety of the histidinehydroxamic acid (Hisha) results in the elimination of the amino-*N* as a donor atom and also a significantly decreased solubility of all the ligand and especially the metal complexes.

The arrangement of the donor atoms in *Z*-Hisha allow the formation of a 5-membered hydroxamate [O,O]-chelate and a 7-membered [N_{imid},N_{hydr}]-chelate. Since, with Ni^{2+} and Zn^{2+} the stability of the latter chelate and also the monodentate coordination of the imidazole-*N* is negligible compared to the stability of the former chelate, hydroxamate-type coordination mode predominates in low stability complexes in these two systems. However, the interaction between Cu^{2+} and *Z*-Hisha is very strong and results in the formation of a high stability metallacrown. This complex provides a good example for the existence of 12-MC-4 type metallacrown with involvement of 5-membered and 7-membered chelates.

Acknowledgements

This work was supported by the Hungarian Scientific Research Fund (OTKA-NKTH CK77586).

[2] In the case of im-4-Cha, which contains the imidazole-*N* in α-position to the hydroxamate function, the stability constant was determined and ESI-MS support of $[Cu_5H_{-4}L_4]^{2+}$ was obtained in DMSO-water 50:50% (m/m) mixture at $t = 25.0$ °C and $I = 0.20$ M (KCl) in the present work. The obtained log $\beta[Cu_5H_{-4}L_4]^{2+} = 44.11$, $m/z = 408$.

Appendix A. Supplementary data

Supplementary data associated with this article can be found, in the online version, at doi:10.1016/j.poly.2010.08.023.

References

[1] A.F. Chambers, L.M. Matrisian, J. Nat. Canc. Inst. 89 (1997) 1260.
[2] M. Egeblad, Z. Werb, Nat. Rev. Canc. 2 (2002) 161.
[3] D.T. Puerta, M.O. Griffin, J.A. Lewis, D. Romero-Perez, R. Garcia, F.J. Villarreal, S.M. Cohen, J. Biol. Inorg. Chem. 11 (2006) 131.
[4] D.T. Puerta, S.M. Cohen, Curr. Top. Med. Chem. 4 (2004) 3003.
[5] E.M.F. Muri, M.J. Nieto, R.D. Sindelar, J.S. Williamson, Curr. Med. Chem. 9 (2002) 1631.
[6] A. Rossello, E. Nuti, M. Pia Catalani, P. Carelli, E. Orlandini, S. Rapposelli, T. Tuccinardi, S.J. Atkinson, G. Murphy, A. Balsamoa, Bioorg. Med. Chem. Lett. 15 (2005) 2311.
[7] M.S. Finnin, J.R. Donigian, A. Cohen, V.M. Richon, R.A. Rifkind, P.A. Marks, R. Breslow, N.P. Pavletich, Nature 401 (1999) 188.
[8] M. Arnold, D.A. Brown, O. Deeg, W. Errington, W. Haase, K. Herlihy, T.J. Kemp, H. Nimir, R. Werner, Inorg. Chem. 37 (1998) 3920.
[9] A.M. Albrecht-Gary, A.L. Crumbliss, in: H. Sigel, A. Sigel (Eds.), Metal Ions in Biological Systems, vol. 35, Marcel-Dekker, Inc., New York, 1998.
[10] M. Tegoni, M. Remelli, D. Bacco, L. Marchió, F. Dallavalle, Dalton Trans. (2008) 2693.
[11] F. Dallavalle, M. Tegoni, Polyhedron 20 (2001) 2697.
[12] J.J. Bodwin, A.D. Cutland, R.G. Malkani, V.L. Pecoraro, Coord. Chem. Rev. 216-217 (2001) 489.
[13] E. Farkas, I. Kiss, J. Chem. Soc., Dalton Trans. (1990) 749.
[14] P. Buglyó, E.M. Nagy, E. Farkas, I. Sóvágó, D. Sanna, G. Micera, Polyhedron 26 (2007) 1625.
[15] E. Farkas, E. Csapó, P. Buglyó, C.A. Damante, G. Di Natale, Inorg. Chim. Acta 362 (2009) 753.
[16] B. Kurzak, H. Kozlowski, E. Farkas, Coord. Chem. Rev. 114 (1992) 169.
[17] É.A. Enyedy, H. Csóka, I. Lázár, G. Micera, E. Garribba, E. Farkas, J. Chem. Soc., Dalton Trans. (2002) 2632.
[18] E. Farkas, H. Csóka, G. Bell, D.A. Brown, L.P. Cuffe, N.J. Fitzpatrick, W.K. Glass, W. Errington, T.J. Kemp, J. Chem. Soc., Dalton Trans. (1999) 2789.
[19] I. Sóvágó, K. Ősz, Dalton Trans. (2006) 3841.
[20] H. Kozlowski, W. Bal, M. Dyba, T. Kowalik-Jankowska, Coord. Chem. Rev. 184 (1999) 319.
[21] E. Leporati, J. Chem. Soc., Dalton Trans. (1987) 435.
[22] B. Kurzak, K. Bogusz, D. Kroczewska, J. Jezierska, Polyhedron 20 (2001) 2627.
[23] B. Kurzak, A. Kamecka, K. Bogusz, J. Jezierska, Polyhedron 26 (2007) 4345.
[24] B. Kurzak, A. Kamecka, K. Bogusz, J. Jezierska, Polyhedron 26 (2007) 4223.
[25] E. Farkas, D. Bátka, E. Csapó, P. Buglyó, W. Haase, D. Sanna, Polyhedron 26 (2007) 543.
[26] W.L.F. Armarego, D.D. Perrin, Purification of Laboratory Chemicals, fourth ed., Butterworth-Heinemann Press, Oxford, 1999.
[27] G. Gran, Acta Chem. Scand. 4 (1950) 559.
[28] L. Erdey, Gravimetric Methods of Chemical Analysis, Akadémiai Kiadó, Budapest, 1960. p. 431.
[29] H.M. Irving, M.G. Miles, L.D. Pettit, Anal. Chim. Acta 38 (1967) 475.
[30] T. Mussini, A.K. Covington, P. Longhi, S. Rondinini, Pure Appl. Chem. 57 (1985) 865.
[31] L. Zékány, I. Nagypál, in: D.L. Leggett (Ed.), Computational Methods for the Determination of Stability Constants, Plenum Press, New York, 1985, p. 291.
[32] A. Rockenbauer, L. Korecz, Appl. Magn. Reson. 10 (1996) 29.
[33] E. Farkas, D. Bátka, H. Csóka, N.V. Nagy, Bioinorg. Chem. Appl., doi:10.1155/2007/96536.
[34] E. Farkas, T. Kiss, B. Kurzak, J. Chem. Soc., Perkin Trans. 2 (1990) 12.
[35] B. Monzyk, A.L. Crumbliss, J. Org. Chem. 45 (1980) 4670.
[36] E.M. Bianchi, R. Griesser, H. Sigel, Helv. Chim. Acta. 88 (2005) 406.
[37] K. Várnagy, E. Garribba, D. Sanna, I. Sóvágó, G. Micera, Polyhedron 24 (2005) 799.
[38] E. Farkas, É.A. Enyedy, H. Csóka, J. Inorg. Biochem. 79 (2000) 205.
[39] E. Farkas, E. Kozma, M. Pethő, K.M. Herlihy, G. Micera, Polyhedron 17 (1998) 3331.
[40] A. Gergely, I. Sóvágó, Inorg. Chim. Acta 20 (1976) 19.
[41] H. Sigel, R.B. Martin, Chem. Rev. 82 (1982) 385.
[42] I. Török, T. Gajda, B. Gyurcsik, G.K. Tóth, A. Péter, J. Chem. Soc., Dalton Trans. (1998) 1205.
[43] E. Farkas, A. Corona, unpublished results.